Quest for an Optimal Methane Hydrate Formation in the Pores of Hydrolytically Stable Metal–Organic Frameworks

Carlos Cuadrado-Collados, Georges Mouchaham, Luke Daemen, Yongqiang Cheng, Anibal Ramirez-Cuesta, Himanshu Aggarwal, Alexander Missyul, Mohamed Eddaoudi, Youssef Belmabkhout, Joaquin Silvestre-Albero

Quest for an optimal methane hydrates formation in the pores of hydrolytically stable MOFs

Carlos Cuadrado-Collados,[†,⊥] Georges Mouchaham,[‡,⊥] Luke Daemen,[§] Yongqiang Cheng,[§] Anibal Ramirez-Cuesta,[§] Himanshu Aggarwal,[‡] Alexander Missyul,[±] Mohamed Eddaoudi,[‡] Youssef Belmabkhout[¥‡] and Joaquin Silvestre-Albero[†].

[†]Laboratorio de Materiales Avanzados, Departamento de Química Inorgánica-IUMA, Universidad de Alicante, E-03690 San Vicente del Raspeig, Spain

[‡]Functional Materials Design, Discovery & Development Research Group, Division of Physical Sciences and Engineering, King Abdullah University of Science and Technology, Thuwal 23955-6900, Kingdom of Saudi Arabia

[§]Oak Ridge National Laboratory, Spallation Neutron Source, 1 Bethel Valley Road, Oak Ridge, USA

[¥]Chemical and Biochemical Sciences. Green Process Engineering. Mohamed VI Polytechnic University, Lot 660 – Hay Moulay Rachid, 43150 Ben Guerir, Morocco.

[±]CELLS-ALBA Synchrotron, Cerdanyola del Vallés, Barcelona, Spain.

[⊥]These two authors contributed equally.

ABSTRACT: Porous MOFs capable of storing relatively high amount of dry methane (CH_4) in adsorbed phase are largely explored, however solid CH_4 storage in confined pores of MOFs in the form of hydrates is yet to be discovered. Here we report a rational approach to form CH_4 hydrates by taking advantage of the optimal pore confinement in relatively narrow cavities of hydrolytically stable MOFs. Unprecedentedly, we were able to isolate methane hydrate (MH) nanocrystals with a sI structure encapsulated inside MOF pores with an optimal cavity dimension. It was found, that confined nanocrystals require cavities slightly larger than the unit cell crystal size of MHs (1.2 nm), as exemplified in the experimental case study performed on Cr-**soc**-MOF-1 *vs* smaller cavities of Y-**shp**-MOF-5. Under these conditions, the excess amount of methane stored in the pores of Cr-**soc**-MOF-1 in the form of MH was found to be ≈50% larger than the corresponding dry adsorbed amount at 10 MPa. More importantly, the pressure gradient driving the CH_4 storage/delivery process could be drastically reduced compared to the conventional CH_4 adsorbed phase storage on the dry Cr-**soc**-MOF-1 (≤3 MPa vs. 10 MPa)

INTRODUCTION

Nowadays, in spite of the tremendous progress in the discovery and development of highly porous metal-organic frameworks (MOFs), only few works on methane (CH_4) storage fulfilled the department of Energy of USA (DoE) target (gravimetric (0.5 g/g) and volumetric (263 v/v)), albeit at 258 K[1]. Nevertheless, this target is still hardly achievable at relatively higher temperatures. Obviously, the main challenges are mainly governed by the progress in materials science, particularly with regards to the discovery of 3D highly porous networks with high control on pore confinements and functionalities.

In general, MOFs, porous organic polymers (POPs) and activated carbon (AC) materials are the main families of materials in the pool potentially capable to achieve high methane storage in the adsorbed phase form in dry conditions, although at pressures as high as 8.0-10.0 MPa.[2-6] A potential alternative approach to enhance methane storage is the so-called solid methane storage, i.e. the storage of methane in crystalline hydrate structures similar to those found in nature.[7] Although that bulk hydrates suffer from a low yield, due to the limited gas-liquid interface, the experience made on AC showed that confining the CH_4 hydrates assembly in nanoporous solids allows to increase the water-to-hydrate conversion at relatively low pressure, while shortening the nucleation time and growth kinetics.[8-11] Although this first development step for CH_4 storage via CH_4 hydrates in porous materials was encouraging, the nucleation process is still not understood.

Due to their high modularity in terms of porous structure and surface chemistry, MOFs stand as model versatile platform to shed light on the CH_4 hydrates nucleation process in relation to specific pore size and shape in porous media, with the ultimate objective to promote gas hydrate formation.[12-15] This opportunity could be a key in understanding the methane hydrates formation in porous materials, in general, and in ordered-crystalline porous materials, in particular. Early stage studies on solid CH_4 storage was carried out on a plethora of porous materials including MOFs, but to the best of our knowledge no report showed gas hydrates growth inside the cavities of MOFs.[16,17] In fact, it was reported that highly hydrophilic mesoporous MOFs (e.g., MIL-100(Fe)) promote strong water-network interactions, with the associated structural blocking. Conversely, hydrophobic MOFs (e.g., ZIF-8) promote gas hydrate formation exclusively in the external surface, inner

cavities remaining fully available for gas physisorption. Thus, promoting the formation of gas hydrates within MOFs cavities is a challenge yet to be addressed and early stage studies are of high importance to delineate the potential of CH_4 hydrates technology. Accordingly, prior to evaluating the performance of this technology using MOFs *vs* other CH_4 storage approaches, standing at different development stages, it is necessary to shed light on the structural properties of MOFs *vs* CH_4 hydrates nucleation potential. In this regard, the use of the adequate MOF, showing appropriate pores' geometry and chemical texture, remains crucial and need to be rationally selected, taking into consideration the often-conflicting factor of hydrolytical stability. The understanding of the nucleation mechanism of isolated, uniform and homogeneously distributed MH nanocrystals within MOF cavities will allow to find pathways to improve methane storage capacity over a narrow pressure window (defined by the formation and dissociation pressures), compared to conventional physisorption processes (i.e., a larger working capacity under less demanding pressure swinging conditions).

Recent studies have shown that reticular chemistry via the design of suitable organic building block allowed the discovery of porous network MOFs with an exceptional water adsorption capacity (up to 200 wt.%).[18,19] The preferential location of the adsorbed water in the form of cluster filling in the inner cavities, the adequate size of these cavities (similar to the MH unit crystal), and the associated strong adsorption potential, anticipates *a priori* a large potential as platforms to promote the nucleation of isolated gas hydrate nanocrystals. To this end, two hydrolytically stable MOFs, Y-**shp**-MOF-5 and Cr-**soc**-MOF-1, have been selected and evaluated for their CH_4 storage performance at high-pressure both under dry adsorption process conditions and water pre-loaded (adsorbed) samples with different amounts of water.

Y-**shp**-MOF-5 (Figure 1a) is a hybrid microporous highly connected rare-earth-based MOF characterized by a relatively intermediate water uptake (up to 0.45 g/g) under a narrow relative humidity range uniquely suitable for moisture control in confined spaces.[18] The Y-**shp**-MOF-5 structure can be viewed as a hexagonal close packing of nonanuclear molecular building blocks, thus forming uniform triangular 1D channels with an opening of 1.2 nm along the *c* axis. Apparent BET surface area is 1550 m^2/g and the total pore volume is 0.63 cm^3/g (see Figures S1-S3 for further details).

Cr-**soc**-MOF-1 (Figure 1b) is built of chromium trimers and large tetratopic organic building blocks and offers an extraordinary CH_4 and water adsorption behavior, in addition to a remarkable chemical stability.[19] Cr-**soc**-MOF-1 has an apparent surface area above 4500 m^2/g, and an exceptional water uptake as high as 1.95 g/g, i.e. nearly 200 wt.%. Cr-**soc**-MOF-1 also possess both cuboidal cages and 1D channels with a pore diameter of ~ 1.5 nm, ~ 1.7 nm, respectively (see Figures S4-S6 for further details). In addition to the hydrolytic stability, the selection of these two MOFs has been motivated by their extraordinary water adsorption capacity accompanied with clusterization phenomenon, together with the dimension of their pores, rather similar (Y-**shp**-MOF-5) or slightly above (Cr-**soc**-MOF-1) the unit crystal size of the methane hydrates (1.2 nm). The main goal would be to shed light on the growth of isolated MH nanocrystals using the different controlled confinement of these two MOFs and evaluate the potential of using each individual cavity of the MOFs studied as a nanoreactor to this end.

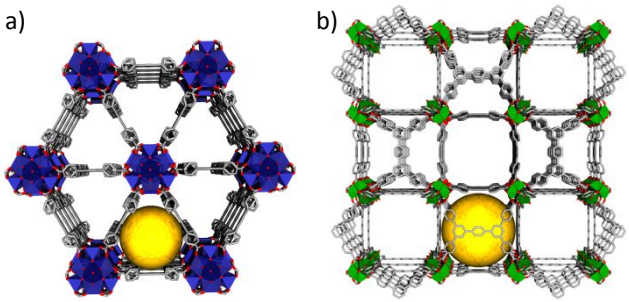

Figure 1. Crystalline structures of a) Y-**shp**-MOF-5 and b) Cr-**soc**-MOF-1. Yellow spheres highlight the triangular channels of Y-**shp**-MOF-5 and the cuboidal cages of Cr-**soc**-MOF-1. Color code: Y, blue; Cr, green; O, red; C, grey. H atoms and counter-ions are not represented for sake of clarity.

RESULTS AND DISCUSSION

High-pressure methane isotherms at 275 K. To evaluate the effect of the water content in the hydrate formation process, high-pressure methane sorption measurements were performed on the two MOFs before and after loading water at different R_w (see Supporting Information). Figure 2 shows the excess methane uptake for (a) Y-**shp**-MOF-5 and (b) Cr-**soc**-MOF-1 samples, both at dry and different R_w, associated to different water pre-loading conditions. As expected, dry MOFs exhibit a type I-like adsorption isotherm with a maximum CH_4 uptake around 12 wt.% (0.12 g/g) at 6-7 MPa, for Y-**shp**-MOF-5, and a larger amount, up to 24 wt.%, at 7-8 MPa for Cr-**soc**-MOF-1.

After measuring the dry isotherms, Y-**shp**-MOF-5 was pre-humidified starting at R_w = 0.3 (60% load) followed by progressive pressurization with CH_4. The main purpose of progressive loading at R_w = 0.3 was to incorporate water first exclusively at the Y^{3+} open metal sites, as primary adsorption sites at low relative humidity.[18] Below 4 MPa, the threshold pressure for methane hydrate formation, the CH_4 adsorption isotherm resembles the original type I, i.e. cavities are partially accessible. Above this pressure some anomalies can be noticed for R_w = 0.3 (mainly at around 6 MPa). Further increase in R_w (R_w = 0.5; 100% load) to saturate the Y-**shp**-MOF-5, followed by a subsequent CH_4 pressurization led to a clear alteration in the CH_4 isotherm shape from the original dry baseline, with a marked hysteresis loop between 5 and 10 MPa. This result clearly reflects some nucleation (upon adsorption) and dissociation (upon desorption) of some confined hydrates. In this particular case, we conclude that the presence of a significant adsorption capacity for methane at low pressures denotes the presence of a significant uptake due to pure physisorption, very probably due to the displacement of water from inner cavities by high-pressure methane. In a final attempt to promote the MH formation, Y-**shp**-MOF-5 was oversaturated with R_w = 0.75 (150% load). However, under these water pre-loaded conditions, the blocking effect is more significant at low pressures, although associated later with a significant hydrate formation at about 3-4 MPa. From all the above-mentioned results and observations, it was found that the cavity dimension of Y-**shp**-MOFs (1.2 nm) is not

favorable to accommodate both water and CH_4 in conditions to allow in turn favorable conditions for MH formation. This is clearly seen for the CH_4 uptake at 10 MPa located below the dry CH_4 baseline for all water pre-loaded experiments.

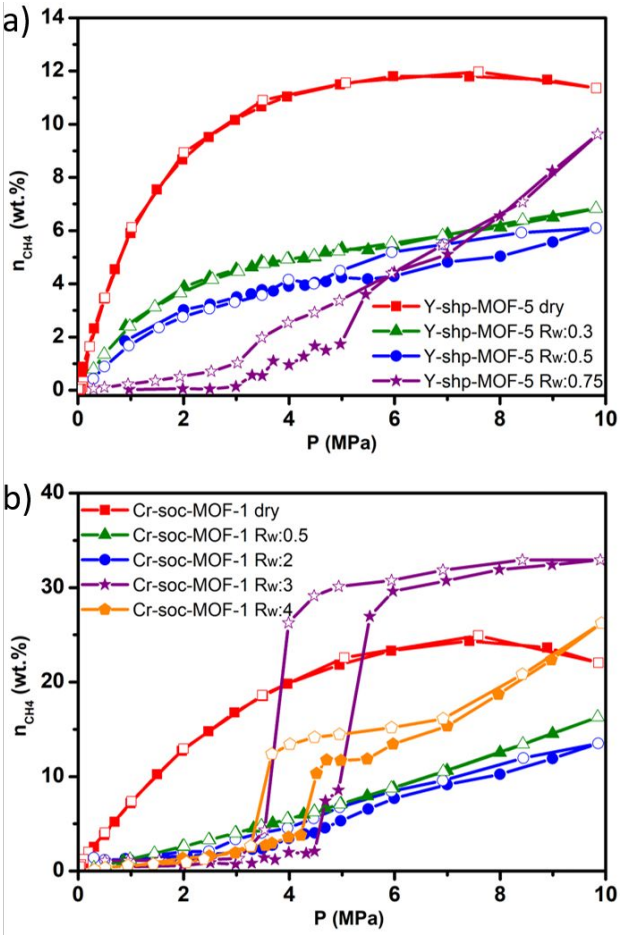

Figure 2. High-pressure excess methane adsorption (full symbols)/desorption (empty symbols) isotherms at 275 K and under different water pre-loaded conditions (Rw corresponds to gram of H_2O per gram of MOF; stands for the ratio of water loaded per gram of sample) for samples (a) Y-**shp**-MOF-5 and (b) Cr-**soc**-MOF-1.

A similar experimental approach was implemented for the Cr-**soc**-MOF-1 (Figure 2b). In this case, the amount of water pre-loaded ranged from under-saturation to over-saturation conditions in similar/close loading percentages as Y-**shp**-MOF-5. Undersaturated and saturated samples (R_w = 0.5 (25% load) and 2 (100% load), respectively) exhibit a complete blocking of the porosity by water with a poor methane uptake over the whole pressure range evaluated. These results anticipate that when the cavities are partially or totally filled with water, methane cannot penetrate the inner cavities and/or interact with water to make hydrate crystals. Interestingly, the scenario changes completely under slight oversaturation conditions. Indeed, the Cr-**soc**-MOF-1 sample pre-loaded with 3 g/g (150% load) exhibits a complete blockage behavior toward methane below 4.5 MPa. However, above this threshold pressure, the methane uptake exhibits two consecutive jumps in a short pressure range to reach an immediate saturation of 33 wt. % at pressures slightly above 6 MPa. Markedly, this abrupt increase in the methane uptake and the shift observed in the desorption branch, associated with a hysteresis loop, are strong evidences for the promotion of gas hydrates formation, with a high water-to-hydrate yield. Compared to previous hydrates confined in activated carbon materials, hydrates confined in MOFs exhibit some peculiar characteristics. While nucleation of gas hydrates in the external surface or in large cavities of carbon materials takes place at 3-4 MPa, larger pressures are required for crystals grown in their narrower cavities.[8] Based on these premises, the shift in the threshold pressure in Cr-**soc**-MOF-1 to 4.5-5 MPa is considered as a clear indication of the preferential nucleation in the inner cavities (nucleation on the external surface can be excluded, except the small step at 4.5 MPa, most probably associated with the MH nucleation at the pore mouth). In addition, the uniform jump between 4.5 MPa and 5.5 MPa suggests that hydrate nanocrystals must be quite uniform, their formation and dissociation taken place in a narrow pressure window. This observation has tremendous implications for a potential application of these materials in methane storage devices since the system can be charged and discharged under less demanding pressure swinging conditions, i.e., it exhibits an ideal working capacity profile. Last but not least, it is important to highlight that the total uptake at 10 MPa constitutes a 50% improvement compared to the dry material (up to 0.33 g/g), this value being among the best reported in the literature so far for carbon materials and MOFs.[2,3] A further increase in the amount of water pre-adsorbed to R_w = 4 becomes detrimental and seems to limit the process of MH growth. Although a significant MH formation is preserved in the pressure window 3.5-4.5 MPa, the total yield remains quite limited. This last result is another evidence of optimal formation of CH_4 hydrate at R_w=3 for Cr-**soc**-MOF-1. It is important to mention that the purpose of imposing an excess of water surrounding the material while progressively preforming CH_4 pressurization is to trigger the formation of hydrate and drive stoichiometry in favor to natural hydrate formation (1 $CH_4 \cdot 5.75\ H_2O$).

The intensive experimental work carried out and summarized above confirm that Y-**shp**-MOF-5 with a pore size similar to the methane hydrate crystal does not promote significantly the water-to-hydrate formation process; most probably due to the steric restrictions in narrow cavities. However, slightly larger cavities, such as those present in Cr-**soc**-MOF-1, accompanied by the appropriate amount of water, can promote hydrate nucleation with a high yield.

Further analysis of the CH_4 storage data allow to access the stoichiometry driving the methane hydrate formation/dissociation at 10 MPa and R_w = 3. In fact, assuming that the whole amount of water participates in the hydrate formation process, gives a value of 1 $CH_4 \cdot 8.0\ H_2O$. Compared to natural hydrates (1 $CH_4 \cdot 5.75\ H_2O$), gas hydrates confined in MOFs exhibit some excess of water, most probably reflecting some limitations in the water-to-hydrate yield. One can assume that 2/3 of the water (2 g/g) are converted to gas hydrate, thus fitting the stoichiometry of the natural hydrates, i.e., $1CH_4 \cdot 5.8H_2O$, whereas 1/3 of water remains unchanged or displaced. The 1/3 residual water left in the pores scenario, could most probably be caused by direct interaction of water with the MOF inner walls (water not prone to make hydrates; yield MH≈66%). The presence of a surface layer of non-freezable water could explain the

obtained results. Such explanation is in close agreement with the case of gas hydrates grown in silica.[20,21] Water displacement at increasing CH_4 pressure could be the most probable scenario to reach the equilibrium of $1CH_4 \cdot 5.8H_2O$ relevant to natural hydrate formation.

Inelastic neutron scattering (INS) experiments. A potential technique to assess the presence of gas hydrates, even when they are confined in narrow cavities, is inelastic neutron scattering (INS). INS is a suitable technique to evaluate the dynamic of atoms, especially vibrational and rotational modes. Due to the large neutron scattering cross section of hydrogen, INS is ideal to probe not only structural dynamics but also rotational tunneling of entrapped and isolated CH_4 molecules. In a first approach, the INS spectra were measured on the desolvated MOFs in order to identify the main rotational and vibrational modes of the parent structure before proceeding with the methane hydrate evaluation.

Figure 3 shows the INS spectra of the bare (a) Y-**shp**-MOF-5 and (b) Cr-**soc**-MOF-1 samples measured at 5 K in the low energy transfer region. The spectra for both samples in the low & mid-energy regions are included in the supporting information (Figures S7 & S8). The low energy transfer region contains the terahertz spectroscopic modes and reveals framework dynamics, whereas the mid-energy region contains the deformation and bending modes from the linker. In the specific case of the Y-**shp**-MOF-5, the INS spectra were also simulated using CP2K calculations (see Figure 3a). INS spectrum of the Y-**shp**-MOF-5 shows two main contributions at ~8 meV and ~50 meV, together with small contributions at ~24 and ~35 meV. As shown in Figure 3a, CP2K calculations are able to reproduce the two main peaks. The contribution at ~8 meV is associated to the ring spinning/flapping and the one at ~50 meV is due to the ring twisting (see animations in Supporting Information).

The low energy transfer region describes a similar spectrum for Cr-**soc**-MOF-1 with main contributions at ~4.5, 8, 15 and 50 meV. The similarity between both INS spectra is due to the presence of similar characteristics in the organic linkers used for both metal-organic frameworks (1,2,4,5-tetrakis(4-carboxyphenyl)benzene-H_4BTEB and 3,3", 5, 5"-tetrakis(4-carboxyphenyl)-p-terphenyl-H_4TCPT, for Y-**shp**-MOF-5 and Cr-**soc**-MOF-1, respectively). Consequently, assignment of low energy contributions coincides with Y-**shp**-MOF-5. Unfortunately, CP2K phonon calculations of Cr-**soc**-MOF-1 could not be completed within reasonable time mainly due to its much larger unit cell (1000 atoms). Regarding the mid-energy region, Figure S7 shows a good fitting between the experimental and predicted spectra. As described above, this region contains the vibrational and librational modes of the organic linker.

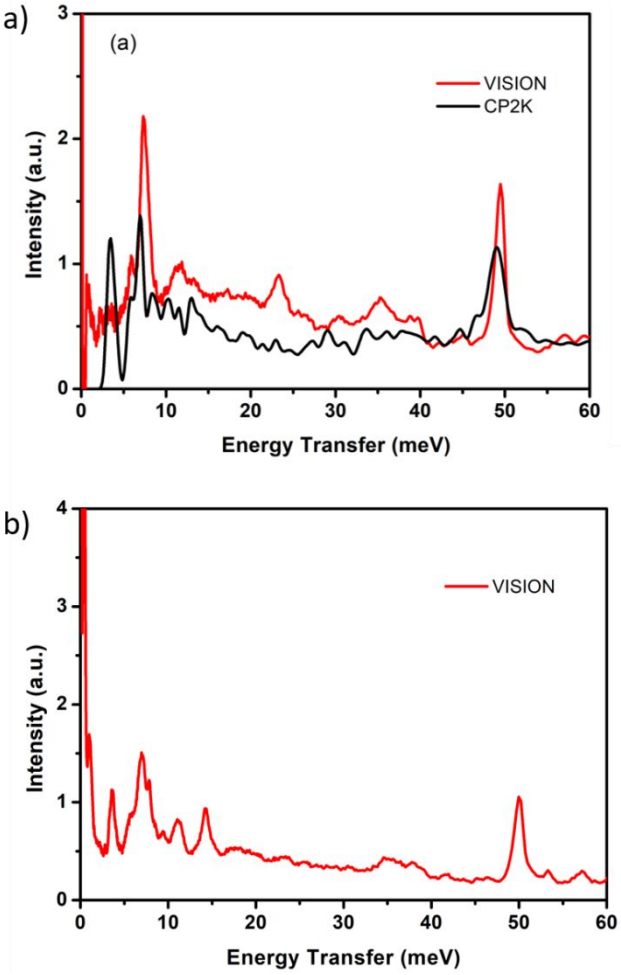

Figure 3. INS spectra of (a) Y-**shp**-MOF-5 and (b) Cr-**soc**-MOF-1 at 5 K in the low energy region.

Upon evaluation of the INS spectra of the desolvated MOFs, the systems were pre-loaded with D_2O up to saturation and subsequently pressurized in the INS chamber with methane up to 6.0 MPa. Upon pressurization at 275 K, the system was cooled down to 5 K to identify potential growth of confined hydrates. D_2O was used instead of H_2O to minimize the background signal (due to parasitic scattering) and get a better imagine of the tunneling transitions in isolated methane molecules. Figures S9 & S10 show the low energy INS spectra of the original, D_2O-supplied, and pressurized systems under dry and wet-conditions. Since the background signal from methane is really broad and wash-out the INS spectrum, Figure 4 shows the final spectra after subtraction of the methane background for (a) Y-**shp**-MOF-5 and (b) Cr-**soc**-MOF-1 materials at 5 K.

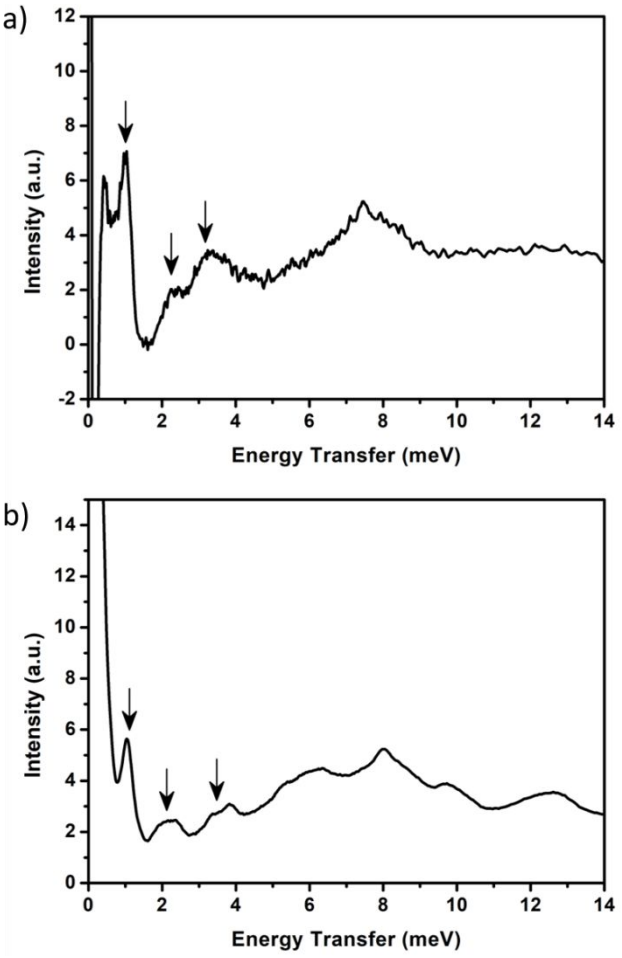

Figure 4. Inelastic neutron scattering (INS) spectra for (a) Y-**shp**-MOF-5 loaded with D_2O R_w=0.5 and (b) Cr-**soc**-MOF-1 loaded with D_2O R_w = 2 at 5 K and under high-pressure methane (6 MPa).

INS spectra of the Y-**shp**-MOF-5 (Figure S9) does not allow to categorize the methane hydrate formation. Only after a background subtraction of the D_2O-loaded MOF and the adsorbed but unreacted CH_4 background (Figure 4a), the low energy transfer region allows to identify peaks at E = 0.96 meV (7.98 cm^{-1}), E = 2.3 meV (18.54 cm^{-1}) and E = 3.3 meV (26.61 cm^{-1}), attributed to the rotational transitions from the ground state to the first and second excitation states, $J = 0 \rightarrow J = 1$, (J = rotational quantum number), $J = 1 \rightarrow 2$, and $J = 0 \rightarrow 2$, respectively. These contributions perfectly fit with the ones observed for natural hydrates.[22] These rotational transitions of the methane molecule are in agreement with an almost free rotor (E = 1.31 meV) due to their entrapped & isolated nature (interaction between methane molecules in different cages must be rather weak). However, the tinny signal observed for Y-**shp**-MOF-5 clearly reflects a low water-to-hydrate yield, in close agreement with the high-pressure measurements described and discussed in detail above. Compared to previous measurements shown in the literature, Y-**shp**-MOF-5 shows an additional contribution at 0.5 meV, most probably due to the defective nature of these confined nanocrystals.

Conversely, the INS data analysis demonstrated completely different results for Cr-**soc**-MOF-1 (Figure 4b). Under saturation conditions and 5 K, the D_2O-loaded MOF pressurized with CH_4 exhibits well-defined methane hydrate contributions at E = 1.00 meV, E = 2.3 meV and E = 3.4 meV (see arrows), thus reflecting a large conversion yield. These results constitute a clear experimental proof about the role of Cr-**soc**-MOF-1 as a host structure to promote optimal condition for the nucleation and growth of confined hydrates. In contrast, the same conditions, these processes are limited in Y-**shp**-MOF-5 due to the presence of a smaller size cavities.

Synchrotron X-ray powder diffraction measurements (SXRPD). In order to evaluate further the observed methane hydrates growth, Y-**shp**-MOF-5 and Cr-**soc**-MOF-1 have been evaluated at the MSPD station at the ALBA synchrotron (Spain) under operando conditions (λ = 0.4135 Å). Figure 5 shows the SXRPD patterns for both samples before and after dosing high-pressure methane (due to the characteristics of the experimental setup, the maximum testing pressure was 4.0 MPa). As it can be observed, in the absence of methane both samples exhibit the characteristic peaks of the studied MOF framework together with some additional peaks (once at 263 K) due to the nucleation and growth of hexagonal ice crystals (I_h). These peaks can be clearly assignable at 2 theta = 6.0, 6.4 and 6.9º.

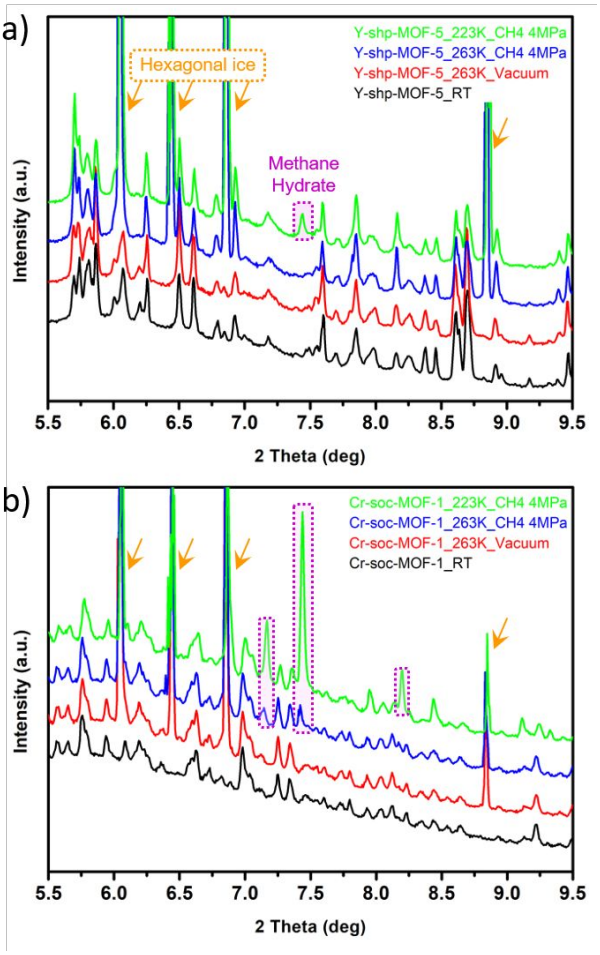

Figure 5. Synchrotron X-ray powder diffraction (SXRPD) patterns for (a) Y-**shp**-MOF-5 loaded with H_2O R_w=0.75 and (b) Cr-**soc**-MOF-1 loaded with H_2O R_w = 3 at different temperatures before and after dosing high-pressure methane (4 MPa).

Upon pressurization with CH_4 up to 4.0 MPa and 263 K, the SXRPD patterns did not show significant changes for Y-**shp**-MOF-5 sample, whereas a small contribution attributed to methane hydrate formation (sI structure) can be appreciated for Cr-**soc**-MOF-1 at 2 theta = 7.4 º. These findings are in good agreements with the behavior of the high-pressure isotherms (adsorption branch) below 4.0 MPa (under these conditions methane hydrate formation is rather limited for both samples as seen in Figure 2). To overcome the set-up pressure limitation, we deliberately attempted shifting of the methane hydrate formation to lower than 4.0 MPa by decreasing the temperature to 223 K. Indeed, in such conditions, Figure 5 shows unambiguously the promotion of the sI structure (main contributions at 2 theta = 7.2, 7.4 and 8.2º), the extend of the water-to-hydrate process being significant for Cr-**soc**-MOF-1. However, the same experiment in Y-**shp**-MOF-5 sample only gives rise to a low contribution (see marked region), thus corroborating previously demonstrated evidence using INS. In other words, these results constitute an additional experimental evidence that Cr-**soc**-MOF-1 is able to promote the methane hydrate formation with a high yield. These crystals have the sI structure, whereas under similar experimental conditions Y-**shp**-MOF-5 promotes preferentially the formation of hexagonal ice (only a very small fraction of the ice can be converted to methane hydrate). Rietveld refinement calculations confirm that upon pressurization with CH_4 additional molecules are accommodated in the cavities of Cr-**soc**-MOF-1 pre-loaded with H_2O. Assuming that these additional molecules correspond to methane (unfortunately SXRPD data does not allow to distinguish between water and methane inside cavities), the confined hydrates will have a stoichiometry of $1CH_4{\cdot}4.4H_2O$. The calculated stoichiometry for the confined hydrates is rather similar to the natural system, although with some water deficiency, most probably associated with the presence of confined, non-freezable, water. In addition, these calculations for Cr-**soc**-MOF-1 predict the presence of additional ice (24%) and methane hydrates (13%) in the external surface and/or at the pore mouth, in agreement with the excess of water pre-loaded (oversaturation conditions).

Phase diagram for the confined methane hydrates. Knowing the pressure threshold for the methane hydrate nucleation and growth, and the dissociation pressure, both values from the high-pressure isotherms, these two processes can be compared with the phase diagram for bulk hydrates (Figure S11).[23,24] As expected, under confined conditions the nucleation and growth process does not follow thermodynamics, i.e. higher pressures are required to promote methane hydrate formation at a given temperature (metastable conditions). As shown in Figure S11, there is a clear trend between the required pressure for nucleation and the pore size of the host structure, independently of the nature of the nanoporous system, i.e., activated carbon or metal-organic framework. In fact, Cr-**soc**-MOF-1 and Y-**shp**-MOF-5 follow the expected tendency for their pore size with the pressure threshold to promote nucleation growing from Cr-**soc**-MOF-1 to Y-**shp**-MOF-5 (these values correspond to the formation of the first nuclei, independently of the obtained yield). On the contrary, experimental results show that hydrate dissociation is indeed under equilibrium conditions, i.e., the pressure threshold is independent of the host structure (chemical nature and porous structure).

In conclusion, the combination of high-pressure adsorption measurements, INS and SXRPD experiments allowed to shed light on the role of pore size control for promoting gas hydrates formation in the pores of MOFs. It was found that Cr-**soc**-MOF-1 combines a proper porous structure (cuboidal cages and 1D channels with an average pore size of ca. 1.6 nm) and surface chemistry to promote the nucleation of isolated methane hydrates with a sI structure. We hypothesize that high water-to-hydrate yield requires slight oversaturation conditions which will in turn promote nucleation at the pore mouth (small step at 4.5 MPa). Further maintaining high CH_4 pressure will allow to propagate nucleation to the inner cavities as inferred from the drastic jump at 5.0 MPa. Under these conditions and assuming the stoichiometry of the natural hydrates, a conversion around 66% can be estimated. The final uptake at 10.0 MPa constitutes a 50% improvement compared to the dry material. Most importantly, this excess uptake (0.33 g/g) can be loaded and released within a narrow working capacity pressure window (only 2.5 MPa). In contrast, the absence of these characteristics in Y-**shp**-MOF-5 precludes the formation of confined methane hydrates with an insignificant yield.

This work represents a highly encouraging step in the development of solid methane storage in MOFs in particular and ordered porous materials in general. Further work will be dedicated to explore isostructural hydrolytic MOFs, with a larger pore sizes, for solid methane storage (SMS).

ASSOCIATED CONTENT

Supporting Information. Experimental and modelling details are included in the Supporting Information. Furthermore, INS spectra for the bare MOFs and the materials are D_2O loading and pressurization with CH_4 at 6.0 MPa are also included.

The Supporting Information is available free of charge on the ACS Publications website.

AUTHOR INFORMATION

Corresponding Author

* Email: joaquin.silvestre@ua.es
* Email: youssef.belmbkhout@um6P.ma

Actual address of G. M.: Institut des Matériaux Poreux de Paris, UMR 8004 CNRS, Ecole Normale Supérieure, Ecole Supérieure de Physique et de Chimie Industrielles de Paris, PSL Université , 75005 Paris, France.

ORCID

Georges Mouchaham: 0000-0001-8696-9733
Carlos Cuadrado-Collados: 0000-0002-4938-2228
Yongqiang Q. Cheng: 0000-0002-3263-4812
Anibal J. Ramirez-Cuesta: 0000-0003-1231-0068
Aleksandr Missyul: 0000-0002-0577-4481
Mohamed Eddaoudi: 0000-0003-1916-9837
Youssef Belmabkhout: 0000-0001-9952-5007
Joaquin Silvestre-Albero: 0000-0002-0303-0817

Author Contributions

All authors proofread and approved the final version of this manuscript for submission.

Notes

No competing financial interests have been declared.

ACKNOWLEDGMENT

G.M, M.E and Y.B thank Aramco sponsored research fund (contract. 66600024505). We would like also to acknowledge the support by King Abdullah University of Science and Technology. J.S.A would like to acknowledge financial support from the MINECO (MAT2016-80285-p), Generalitat Valenciana (PROMETEOII/2014/004), Oak Ridge beam time availability (Project IPTS-20859.1) and Spanish ALBA synchrotron (Project 2020014008).

REFERENCES

(1). Alezi, D.; Belmabkhout, Y.; Suyetin, M.; Bhatt, P.M.; Weselinski, L.J.; Solovyeva, V.; Adil, K.; Spanopoulos, I.; Trikalitis, P.N.; Emwas, A.-H.; Eddaoudi, M. MOF Crystal Paving the Way to Gas Storage Needs: Aluminum-Based soc-MOF for CH_4, O_2, and CO_2 Storage. *J. Am. Chem. Soc.*, **2015**, *137*, 13308-13318.

(2) Peng, Y.; Krungleviciute, V.; Eryazici, I.; Hupp, J.T.; Farha, O.K.; Yildirim, T. Methane Storage in Metal-Organic Frameworks: Current Records, Surprise Findings, and Challenges. *J. Am. Chem. Soc.* **2013**, *135*, 11887-11894.

(3) Casco, M.E.; Martinez-Escandell, M.; Gadea-Ramos, E.; Kaneko, K.; Silvestre-Albero, J.; Rodríguez-Reinoso, J. High-Pressure Methane Storage in Porous Materials: Are Carbon Materials in the Pole Position?. *Chem. Mater.* **2015**, *27*, 959-964.

(4) Tian, T.; Zeng, Z.; Vulpe, D.; Casco, M.E.; Divitini, G.; Midgley, P.A.; Silvestre-Albero, J.; Tan, J-C.; Moghadam, P.Z.; Fairen-Jimenez, D. A Sol-Gel Monolithic Metal-Organic Framework with Enhanced Methane Uptake. *Nature Mater.* **2018**, *17*, 174-179.

(5) Connolly, B.M.; Aragones-Anglada, M.; Gandara-Loe, J.; Danaf, N.A.; Lamb, D.C.; Mehta, J.P.; Vulpe, D.; Wuttke, S.; Silvestre-Albero, J.; Moghadam, P.Z.; Wheatley, A.E.H.; Fairen-Jimenez, D. Tuning porosity in macroscopic monolithic metal-organic frameworks for exceptional natural gas storage. *Nature Commun.*, **2019**, *10*, 2345.

(6) Jia, J.; Chen, Z.; Jiang, H.; Belmabkhout, Y.; Mouchaham, G.; Aggarwal, H.; Adil, K.; Abou-Hamad, E.; Czaban-Jozwiak, J.; Rachid Tchalala, M.; Eddaoudi, M. Extremely Hydrophobic POPs to Access Highly Porous Storage Media and Capturing Agent for Organic Vapors. *Chem*, **2019**, *5*, 180-191.

(7) Sloan, E.D. Fundamental Principles and Applications of Natural Gas Hydrates. *Nature* **2003**, *426*, 353-359.

(8) Casco, M.E.; Silvestre-Albero, J.; Ramirez-Cuesta, A.J.; Rey, F.; Jordá, J.L.; Bansode, A.; Urakawa, A.; Peral, I.; Martínez-Escandell, M.; Kaneko, K.; Rodríguez-Reinoso, F. Methane Hydrate Formation in Confined Nanospace Can Surpass Nature. *Nature Commun.* **2015**, *6*, 6432.

(9) Cuadrado-Collados, C.; Majid, A.A.A.; Martinez-Escandell, M.; Daemen, L.L.; Missyul, A.; Koh, C.; Silvestre-Albero, J. Freezing/Melting of Water in the Confined Nanospace of Carbon Materials: Effect of an External Stimulus. *Carbon* **2020**, *158*, 346-355.

(10) Siangsai, A.; Rangsunvigit, P.; Kitiyanan, B.; Kulprathipanja, S.; Linga, P. Investigation on the Roles of Activated Carbon Particle Sizes on Methane Hydrate Formation and Dissociation. *Chem. Eng. Sci.*, **2015**, *126*, 383-389.

(11) Celzard, A.; Mareché, J.-F. Optimal Wetting of Active Carbons for Methane Hydrate Formation. *Fuel*, **2005**, *85*, 957-966.

(12) Zhou, H.-C.; Long, J.R.; Yaghi, O.M. Introduction to Metal-Organic Frameworks. *Chem. Rev.* **2012**, *112*, 673-674.

(13) Kaskel, S. (Ed.), The Chemistry of Metal-Organic Frameworks: Synthesis, Characterization and Applications, Wiley-VCH, **2016**.

(14) Eddaoudi, M.; Kim, J.; Rosi, N.; Vodak, D.; Wachter, J.; O´Keeffe, M.; Yaghi, O.M. Systematic Design of Pore Size and Functionality in Isoreticular MOFs and Their Application in Methane Storage. *Science*, **2002**, *295*, 469-472.

(15) Furukawa, H.; Ko, N.; Go, Y.B.; Aratani, N.; Choi, S.B.; Choi, E.; Yazaydin, A.O., Snurr, R.Q.; O´Keeffe, M.; Kim, J.; Yaghi, O.M. Ultrahigh Porosity in Metal-Organic Frameworks. *Science*, **2010**, *329*, 424-428.

(16) Casco, M.E.; Rey, F.; Jorda, J.L.; Rudic, S.; Fauth, F.; Martínez-Escandell, M.; Rodríguez-Reinoso, F.; Ramos-Fermández, E.V.; Silvestre-Albero, J. Paving the Way for Methane Hydrate Formation on Metal-Organic Frameworks (MOFs). *Chem. Sci.* **2016**, *7*, 3658-3666.

(17) Mu, L.; Liu, B.; Liu, H.; Yang, Y.; Sun, C.; Chen, G. A Novel Method to Improve the Gas Storage Capacity of ZIF-8. *J. Mater. Chem.*, **2012**, *22*, 12246-12252.

(18) AbdulHalim, R.G.; Bhatt, P.M.; Belmabkhout, Y.; Shkurenko, A.; Adil, K.; Barbour, L.J.; Eddaoudi, M. A Fine-Tuned Metal-Organic Framework for Autonomous Indoor Moisture Control. *J. Am. Chem. Soc.* **2017**, *139*, 10715-10722.

(19) Abtab, S.M.T.; Alezi, D.; Bhatt, P.M.; Shkurenko, A.; Belmabkhout, Y.; Aggarwal, H.; Weselinski, L.J.; Alsadun, N.; Samin, U.; Hedhili, M.N.; Eddaoudi, M. Reticular Chemistry in Action: A Hydrolytically Stable MOF Capturing Twice Its Weight in Adsorbed Water. *Chem* **2018**, *4*, 94-105.

(20) Bai, D.; Chen, G.; Zhang, X.; Wang, W. Microsecond Molecular Simulations of the Kinetic Pathways of Gas Hydrate Formation from Solid Surfaces. *Langmuir*, **2011**, *27*, 5961-5967.

(21) Liang, S.; Rozmanov, D.; Kusalik, P.G. Crystal Growth Simulations of Methane Hydrates in the Presence of Silica Surfaces. *Phys. Chem. Chem. Phys.*, **2011**, *13*, 19856-19864.

(22) Gutt, C.; Asmussen, B.; Press, W.; Merkl, C.; Casalta, H.; Greinert, J.; Bohrmann, G.; Tse, J.S.; Hüller, A. Quantum Rotations in Natural Methane-Clathrates from the Pacific Sea-Floor. *Europhys. Lett.*, **1999**, *48*, 269-275.

(23) Borchardt, L.; Nickel, W.; Casco, M.; Senkovska, I.; Bon, V.; Wallacher, D.; Grimm, N.; Krause, S.; Silvestre-Albero, J. Illuminating Solid-Gas Storage in Confined Spaces - Methane Hydrate Formation in Porous Model Carbons. *Phys. Chem. Chem. Phys.*, **2016**, *18*, 20607-20614.

(24) Handa, Y.P.; Stupin, D., Thermodynamic Properties and Dissociation Characteristics of Methane and Propane Hydrates in 70-A Radius Silica Gel Pores. *J. Phys. Chem.*, **1992**, *96*, 8599-8603.